Elastic and electronic properties of perovskite type superconductor $MgCNi_3$ under pressure

2008 J. Phys.: Condens. Matter 20 325228

(http://iopscience.iop.org/0953-8984/20/32/325228)

IOP PUBLISHING JOURNAL OF PHYSICS: CONDENSED MATTER

J. Phys.: Condens. Matter **20** (2008) 325228 (7pp) doi:10.1088/0953-8984/20/32/325228

Elastic and electronic properties of perovskite type superconductor $MgCNi_3$ under pressure

Wei Zhang[1], **Xiang-Rong Chen**[1,2,4], **Ling-Cang Cai**[3] **and Fu-Qian Jing**[1,3]

[1] School of Physical Science and Technology, Sichuan University, Chengdu 610064, People's Republic of China

[2] International Centre for Materials Physics, Chinese Academy of Sciences, Shenyang 110016, People's Republic of China

[3] Laboratory for Shock Wave and Detonation Physics Research, Institute of Fluid Physics, Chinese Academy of Engineering Physics, Mianyang 621900, People's Republic of China

E-mail: xrchen@126.com

Received 20 April 2008, in final form 7 May 2008
Published 18 July 2008
Online at stacks.iop.org/JPhysCM/20/325228

Abstract

The elastic, electronic and some thermodynamic properties of the non-oxide perovskite type superconductor $MgCNi_3$ under pressure are investigated by first-principles calculations. With the local density approximation as well as the generalized gradient approximation for exchange and correlation, the ground state properties and equation of state are obtained, which agree well with both theoretical calculations and experiments. By the elastic stability criteria, we predict that $MgCNi_3$ is not stable above 58.4 GPa. Moreover, from the calculated pressure dependence of Debye temperature and electronic properties, the cause of the enhancement of T_c with the increasing pressure is analyzed.

1. Introduction

Followed by the discovery of MgB_2 [1], observations of superconductivity in another intermetallic compound $MgCNi_3$ (with a critical temperature T_c of 8 K) [2] have aroused great interest among scientists for its many puzzling physical properties. The compound has the classical cubic perovskite structure with space group $Pm\bar{3}m$. In the crystal structure of $MgCNi_3$, the atoms occupy the positions: Mg (0; 0; 0), C (1/2; 1/2; 1/2) and Ni (0; 1/2; 1/2). The high proportion of Ni atoms in the unit cell suggests the possibility of magnetic interactions, which may play a dominant role in explaining the superconductivity [2].

Electronic structure calculations of $MgCNi_3$ [3–8] showed a large narrow density of states (DOS) peak in the vicinity of the Fermi level (E_F). The DOS at E_F is not large enough to induce magnetic instability [5], but is associated with the superconducting properties [7]. Since the peak is located just below E_F, substitution in $MgCNi_3$ is expected to change its electronic properties significantly. Numerous efforts [9–17] have been made with hole-doped $MgCNi_3$ in an attempt to shift the Fermi level, thereby leading an increase of the DOS at E_F, whereupon T_c was found to decrease. Using pressure, some groups successfully enhanced the T_c, but the cause is still controversial. Kumary *et al* [9] considered that the increase in T_c with pressure is due to a lattice softening or a structural phase transition. Yang *et al* [18] thought it can be explained mainly by the increase of DOS with pressure, while Garbarino *et al* [19] speculated that the increase of T_c is due to a reduction of the magnetic character.

In addition, some experiments have been performed for such a complicated system under high pressure. By means of synchrotron x-ray powder diffraction, Loa *et al* [20] investigated the structural stability of $MgCNi_3$ up to 30 GPa, Zhang *et al* [21] and Kumar *et al* [22] studied the structural behavior of $MgCNi_3$ at pressures up to 22 and 32 GPa, respectively. They concluded that the structure of the compound remains in the $Pm\bar{3}m$ cubic symmetry throughout the applied pressure range. However, there are significant uncertainties in the experimental compressibility

[4] Author to whom any correspondence should be addressed.

data of $MgCNi_3$ and whether the compound is stable under a pressure higher than 32 GPa remains unknown.

In this work, we focus on the structural, elastic, electronic and thermodynamic properties of $MgCNi_3$ under pressures up to 60 GPa by using first-principles calculations. The elastic properties of $MgCNi_3$ under high pressure are investigated for the first time, from which we will investigate its mechanical stability. Moreover, from the obtained pressure dependences of the Debye temperature and the electronic properties of $MgCNi_3$, we will make an analysis of the increase in T_c with pressure. In section 2, we give a brief description of the theoretical method. The results of structural, elastic, electronic and thermodynamic properties of $MgCNi_3$ under pressure are presented in section 3. A conclusion is drawn in the last section.

2. Theoretical methods

2.1. Total energy electronic structure calculations

In the electronic structure calculations, the ultrasoft pseudopotentials introduced by Vanderbilt [23] have been employed for all the ion–electron interactions, together with both the local density approximation (LDA) proposed by Vosko *et al* [24] and the generalized gradient approximation (GGA) [25] for the exchange–correlation function. A plane-wave basis set with energy cut-off 400 eV is applied. Pseudo-atomic calculations are performed for Mg 3s2p, C 2s2p and Ni 4s3d. For the Brillouin zone sampling, we use a $8 \times 8 \times 8$ Monkhorst–Pack mesh. The self-consistent convergence of the total energy is 10^{-6} eV/atom. Hydrostatic pressure, coupled with the variable cell approach, is applied within the Parrinello–Rahman method [26, 27] to perform a full optimization of the cell structure for each target external pressure. All these total energy electronic structure calculations are implemented through the Cambridge Serial Total Energy Package (CASTEP) code [28, 29].

2.2. Elastic properties

The elastic stiffness tensor is related to the stress tensor and the strain tensor by Hooke's law. Since the stress and strain tensors are symmetric, the most general elastic stiffness tensor has only 21 non-zero independent components. For a cubic crystal, these are reduced to three components, i.e. C_{11}, C_{12}, and C_{44}. These elastic stiffness coefficients (namely the elastic constants) can be determined by computing the stress generated by applying a small strain to an optimized unit cell [30].

The Debye temperature may be estimated from the average sound velocity V_m [31]

$$\Theta = \frac{h}{k}\left[\frac{3n}{4\pi}\left(\frac{N_A\rho}{M}\right)\right]^{1/3} V_m, \tag{1}$$

where h is Planck's constants, k is Boltzmann's constant, N_A is Avogadro's number, n is the number of atoms per formula unit, M is the molecular mass per formula unit, ρ is the density, and V_m is obtained from [31]

$$V_m = \left[\frac{1}{3}\left(\frac{2}{V_s^3} + \frac{1}{V_l^3}\right)\right]^{-1/3}, \tag{2}$$

where V_s and V_l are the shear and longitudinal sound velocities, respectively.

For a cubic structure $MgCNi_3$, the bulk modulus B and the shear modulus G are taken as

$$B = (C_{11} + 2C_{12})/3 \tag{3}$$

$$G = (3C_{44} + C_{11} - C_{12})/5. \tag{4}$$

Then the Young's modulus E and the Poisson's ratio σ are given by

$$E = \frac{9BG}{3B + G} \tag{5}$$

$$\sigma = \tfrac{1}{2}(1 - E/3B). \tag{6}$$

The shear and longitudinal sound velocities V_s and V_l are obtained from Navier's equation as follows [32]

$$V_s = \sqrt{\frac{G}{\rho}}, \qquad V_l = \sqrt{\left(B + \frac{4}{3}G\right)\Big/\rho}. \tag{7}$$

2.3. Thermodynamic properties

To investigate the thermodynamic properties of $MgCNi_3$, we apply the quasi-harmonic Debye model [33], in which the phononic effect is considered, and the non-equilibrium Gibbs function $G^*(V; P, T)$ takes the form

$$G^*(V; P, T) = E(V) + PV + A_{Vib}(\Theta(V); T) \tag{8}$$

where $E(V)$ is the total energy per unit cell, PV corresponds to the constant hydrostatic pressure condition, $\Theta(V)$ is the Debye temperature, and the vibrational contribution A_{vib} can be written as

$$A_{Vib}(\Theta; T) = nkT\left[\frac{9}{8}\frac{\Theta}{T} + 3\ln(1 - e^{-\Theta/T}) - D(\Theta/T)\right], \tag{9}$$

where the $D(\Theta/T)$ represents the Debye integral, n is the number of atoms per formula unit, and Θ is the Debye temperature defined by equation (1).

By solving the following equation with respect to V

$$\left(\frac{\partial G*(V; P, T)}{\partial V}\right)_{P,T} = 0 \tag{10}$$

one can obtain the thermal expansion coefficient α as follows

$$\alpha = \gamma C_V/(B_T V), \tag{11}$$

where the isothermal bulk modulus B_T, the heat capacity C_V and the Grüneisen parameter γ are expressed as

$$B_T(P, T) = V\left[\frac{\partial^2 G*(V; P, T)}{\partial^2 V^2}\right]_{P,T} \tag{12}$$

$$C_V = 3nk\left[4D(\Theta/T) - \frac{3\Theta/T}{e^{\Theta/T} - 1}\right] \tag{13}$$

$$\gamma = -\frac{d\ln\Theta(V)}{d\ln V}. \tag{14}$$

Table 1. Lattice constants (Å), bulk modulus B_0 (GPa) and its pressure derivative B_0' of $MgCNi_3$ at 0 GPa and 0 K.

	Present work		Other work		
	GGA	LDA	GGA	LDA	Experiments
a	3.833	3.752	3.83[a], 3.813[b], 3.82[c]	3.713[b], 3.74[c], 3.76[d]	3.810[e], 3.81[f]
B_0	170.4	203.2	172.2[a], 168.4[b], 180.5(13)[e]	202.5[b], 210[g], 202[h]	184(5)[e], 156.9[f], 267.8(7)[i]
B_0'	4.49	4.42	4.25[b], 4.12(5)[e]	4.20[b], 4.49[h]	2.9(5)[e], 9.8[f], 4[i]

[a] Reference [36]; [b] Reference [35]; [c] Reference [37]; [d] Reference [38]; [e] Reference [20]; [f] Reference [22]; [g] Reference [9]; [h] Reference [39]; [i] Reference [21].

3. Results and discussion

3.1. Structure and equation of state

For the non-oxide perovskite type superconductor $MgCNi_3$, a series of lattice constants a are set to obtain the total energy E and the corresponding primitive cell volume V through both the GGA and the LDA schemes, and then the obtained E–V data are fitted to the Birch–Murnaghan equation of state (EOS) [34]. In table 1, the obtained equilibrium lattice constants a, zero-pressure bulk modulus B_0 and its pressure derivative B_0' are summarized, together with the available experimental data [20–22] and other theoretical results [9, 35–39]. It is easily found that almost all the theoretical calculations for the lattice constants by GGA are overestimated, and those by LDA are underestimated. The calculated results by GGA are a somewhat better than those by LDA.

We note that there are great discrepancies among the experimental and theoretical data. Through the EDXRD experiment, Zhang *et al* [21] reported the zero-pressure bulk modulus B_0 to be 267.8(7) GPa, which is significantly larger than other conclusions both from theory and experiment. The possible reason for this high value may be due to the inaccuracy in estimating the ambient unit cell volume, and as there is no use of pressure medium reported, the distortions induced on the unit cell may be due to the non-hydrostatic stress coupled with local distortions. Furthermore, $B_0' = 9.8$ is given by Kumar *et al* [22], which is also distinctly larger than other data. Our calculations are in agreement with most of them. In figure 1, we illustrate the normalized cell volume dependence with pressure for $MgCNi_3$, together with the experimental data of $P = 0$–28 GPa [19] and $P = 0$–22 GPa [21]. Our results from both LDA and GGA methods are in good agreement with the experimental data by Kumar *et al* [22] at low pressure (<20 GPa), while at higher pressure (>20 GPa), the LDA results seem to be better than the GGA results. There are large discrepancies between our results and the experimental data by Zhang *et al* [21], especially at higher pressures.

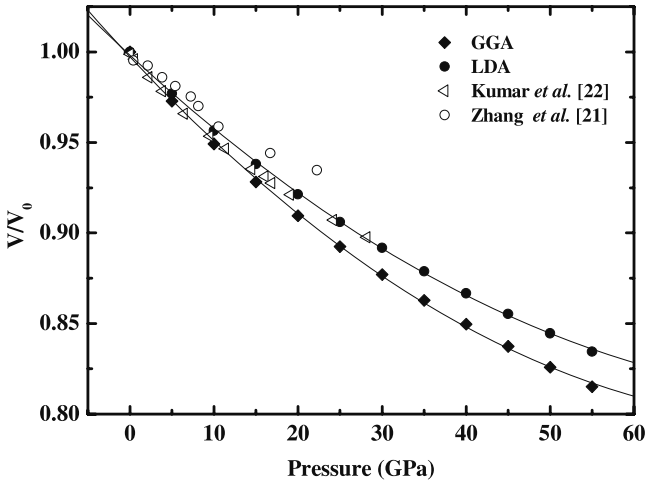

Figure 1. Calculated equation of state of $MgCNi_3$ together with the experimental data from Zhang *et al* [21] and Kumar *et al* [22].

3.2. Elastic constants

The elastic constants C_{11}, C_{12}, and C_{44} of $MgCNi_3$ at 0 GPA and 0 K are listed in table 2. It can be seen that our calculations are consistent with those reported by Vaitheeswaran *et al* [35], who performed their calculations by the all-electron full-potential linear muffin-tin orbital (FP-LMTO) method. Due to an underestimate of the lattice constant, the elastic constant calculated by LDA are larger than those by GGA. Since C_{11}, C_{12} and C_{44} comprise the complete set of elastic constants for a cubic system, the bulk modulus B, Young's modulus E, shear modulus G and Poisson ratio υ can thus derived from them. All of these values are also listed in table 2. Our results seem to be better than those by others.

Table 2. Calculated elastic constants (GPa), bulk modulus B (GPa), Young's modulus E (GPa), shear modulus G (GPa), and Poisson ratio σ at 0 GPa and 0 K.

	C_{11}	C_{12}	C_{44}	B	E	G	σ
GGA	313.2	102.2	40.6	172.6	176.9	66.5	0.329
	342.4[a]	81.4[a]	44.5[a]		204.7[a]	78.9[a]	0.297[a]
LDA	378.5	122.0	43.0	207.5	205.8	77.1	0.335
	421.1[a]	93.3[a]	49.9[a]		247.7[a]	95.5[a]	0.296[a]
Exp					154.15[b]	57.98[b]	0.33[b]

[a] Reference [35]; [b] Reference [40].

The bulk modulus calculated from elastic constants are very close to those obtained from EOS. Compared with the experimental data, the Young's modulus, shear modulus and Poisson ratio obtained are better than those given by Vaitheeswaran *et al* [35], especially for the Poisson ratio, which is almost the same as the experimental result [40]. By analyzing the ratio between bulk modulus and shear modulus, Vaitheeswaran *et al* [35] concluded that $MgCNi_3$ is intermediate between brittle and ductile in nature. The Poisson ratio obtained offered good evidence for such a conclusion; according to Frantsevich's rule [41], the critical value of

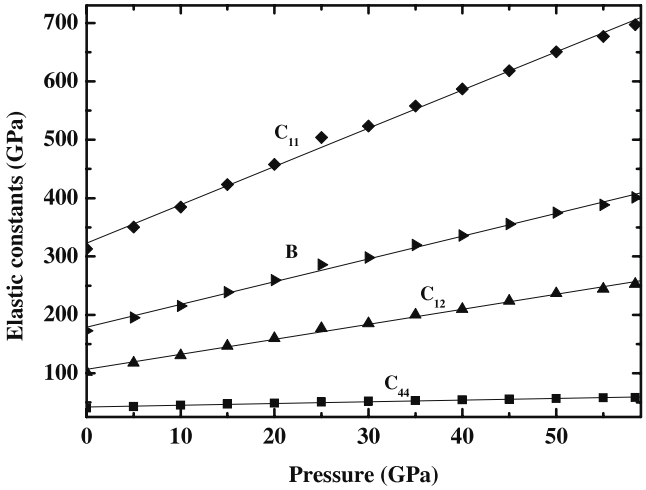

Figure 2. The dependences of elastic constants of $MgCNi_3$ on pressure.

Poisson ratio of a material is 1/3. For brittle materials, the Poisson ratio is less than 1/3, and values larger than 1/3 can be regarded as ductile materials. The Poisson ratio in present work is 0.329 (GGA) and 0.335 (LDA). Both of them are very close to the critical value. Therefore, $MgCNi_3$ indeed locates the exact border between two type materials. However, as the pressure increases the Poisson ratio will become larger than 1/3. This indicates that $MgCNi_3$ will become more ductile under high pressure.

The elastic constants of $MgCNi_3$ under pressure, obtained for the first time, are illustrated in figure 2. It is seen that C_{11}, C_{12}, C_{44} and B_0 increase with the enhancement of pressure. The change of C_{11} is more sensitive to pressure than other three, while C_{44} is the most unresponsive one. As is known, for a cubic crystal, the mechanical stability under isotropic pressure is judged from the following condition [42]

$$\tilde{C}_{44} > 0, \qquad \tilde{C}_{11} > |\tilde{C}_{12}|, \qquad \tilde{C}_{11} + 2\tilde{C}_{12} > 0, \quad (15)$$

where $\tilde{C}_{\alpha\alpha} = C_{\alpha\alpha} - P$ ($\alpha = 1, 4$), $\tilde{C}_{12} = C_{12} + P$. By fitting the $\tilde{C}_{44}$ data to second-order polynomials, we have the following relations

$$\tilde{C}_{44} = 41.0738 - 0.595\,52P - 0.001\,78P^2. \quad (16)$$

When the applied pressure is above 58.4 GPa, $\tilde{C}_{44} > 0$ is no longer fulfilled, indicating that $MgCNi_3$ is not mechanical stable at pressures above 58.4 GPa, which requires a confirmation from experiment. From the obtained elastic constants at 0 GPa and 0 K, the Debye temperature and sound velocities (including longitudinal, shear and average wave velocities) can thus be derived. These are listed in table 3, together with other theoretical results [35] and the experimental data [15, 40, 41, 44] for our comparison. Our results are also better than other theoretical data.

Elasticity, being a fourth-rank tensor property, is anisotropic for a cubic crystal. It is conveniently expressed by the dimensionless parameter $A = [(2C_{44} + C_{12})/C_{11}] - 1$. Through the calculated elastic constants, we can obtain the elastic anisotropic parameter A at different pressures. It is found that the anisotropic parameter A of $MgCNi_3$ remains negative in the entire range of pressure studied and increases with increasing pressure, as opposed to MgO, which becomes elastically isotropic at about 21 GPa [43].

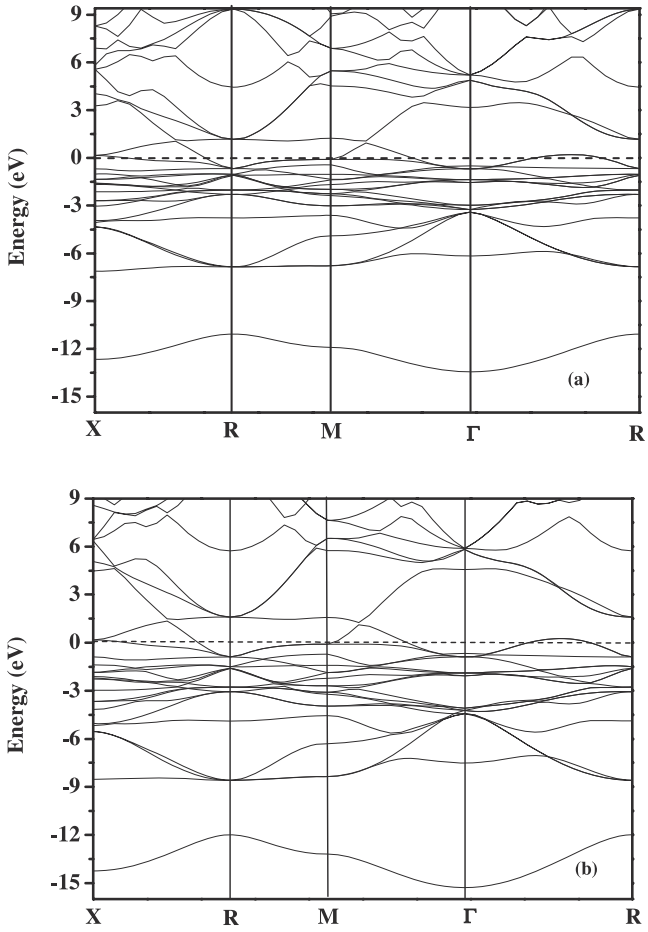

Figure 3. Electronic band structures of $MgCNi_3$ along the high symmetry directions: (a) at 0 GPa, and (b) at 58.4 GPa.

Table 3. Calculated longitudinal, shear and average wave velocity (v_l, v_s and v_m) in m s^{-1} and the Debye temperature Θ in K from the average elastic wave velocity of $MgCNi_3$ at 0 GPa and 0 K.

	V_l	V_m	V_s	Θ
GGA	6458	3654	3259	283.7
	6555[a]	3920[a]	3521[a]	306.2[a]
LDA	6818	3813	3398	302.4
	7199[a]	4324[a]	3874[a]	337[a]
Exp	6090[b]	3070[b]		287[c] 292[d] 351[e]

[a] Reference [35]; [b] Reference [40];
[c] Reference [41]; [d] Reference [44];
[e] Reference [15].

3.3. Electronic band structures

The band structures of $MgCNi_3$ along the symmetry line of the simple cubic Brillouin zone under 0 GPa are shown in figure 3(a). It can be seen that $MgCNi_3$ is metallic with two bands, which have a mainly Ni 3d character crossing the Fermi

Table 4. Densities of states at the Fermi level (states eV^{-1} f.u.$^{-1}$).

	0 GPa			58.4 GPa		
Atoms	s	p	d	s	p	d
Mg	0.0002	0.1178		0.000 04	0.0707	
C	0.0165	0.6126		0.015 4	0.6159	
Ni	0.2019	0.4663	3.871	0.176 7	0.5664	3.392

level along the Γ–M, Γ–R and X–R symmetry directions. Both of them are refined between −0.7 and 1.1 eV, consistent with the results of Shim *et al* [3] and Okoye [36]. The lowest band between −11 and −13.5 eV corresponds to C 2s states, while the dispersive bands between −7 and −4 eV originate mainly from C 2p states. Those bands just below the Fermi level consist of hybridized Ni 3d and C 2p bands but predominantly present Ni 3d character. As the applied pressure is 58.4 GPa, the two valence bands intersect with the Fermi level much more deeply, as is shown in figure 3(b). This behavior is expected to account for a higher T_c in $MgCNi_3$ at higher pressure.

The calculated N (E_F) of the total DOS of $MgCNi_3$ is 5.275 states eV^{-1} f.u.$^{-1}$. This value can also be obtained with other methods: 5.34 (LDA-LMTO) [3], 5.26 (TB-LMTO) [6], 4.99 (LAPW) [7], 6.4 (LDA-FLAPW) [45], and 4.665 (FP-LMTO) [46]. The differences among the previous results of $N(E_F)$ may arise from the different approximations. However, our results maintain good agreement with most of them. Moreover, the individual contributions to the DOS at E_F under 0 and 58.4 GPa are collected in table 4. It is seen that the $N(E_F)$ is mostly contributed by the Ni 3d and C 2p states, and that the contributions from Mg 3s, 2p and C 2s states are too small and can be ignored, which is comparable to the results by Szajek [47]. As the applied pressure is 58.4 GPa, the contributions from C 2p and Ni p states at the Fermi energy show a slight increase. However, the N (E_F) of Ni 3d states reduce by 0.479 states eV^{-1} f.u.$^{-1}$ which will lead a decrease of the $N(E_F)$ of total DOS. It is found that the pressure makes the peaks of the N (E_F) of total DOS below Fermi level move to the lower energies and decreases in height. However, the pressure has little effect on the location of the peak at about 0.1 eV below Fermi level.

3.4. Thermodynamic properties

The dependences of isothermal and adiabatic bulk moduli (B_T, B_S) of $MgCNi_3$ on temperature are illustrated in figure 4. It can be found that B_T and B_S are nearly constant from 0 to 100 K and then decrease almost linearly with increasing temperatures, as is obvious from the relationship $B_S = B_T(1 + \alpha\gamma T)$. B_T and B_S coincide at low temperature and then diverge with rising T. At room temperature, $dB_T/dT = -0.0355$ GPa K^{-1} and $dB_S/dT = -0.0180$ GPa K^{-1}, respectively. It is found that the relationships between bulk modulus and pressure are nearly linear at various temperatures. The bulk modulus decreases with increasing temperature at a given pressure and increases with increasing pressure at a given temperature. These results are due to the fact that the effect of increasing pressure on the material is the same as that of decreasing temperature on it.

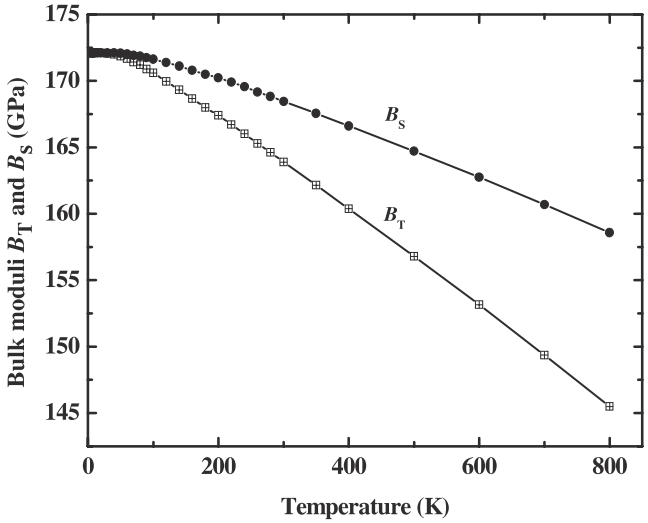

Figure 4. Temperature dependence of isothermal (B_0) and adiabatic (B_S) zero-pressure bulk modulus for $MgCNi_3$.

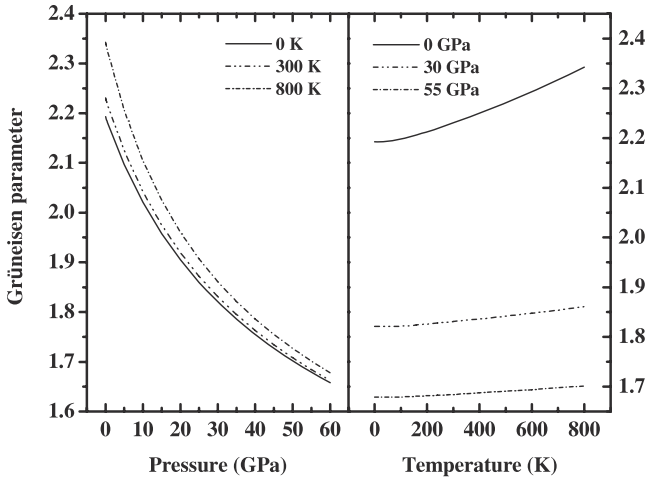

Figure 5. Pressure (left) and temperature (right) dependences of the Grüneisen parameter γ for $MgCNi_3$.

The calculated heat capacity C_V at ambient conditions is 118.8 J mol^{-1} K^{-1}, a good agreement with the experimental value 111.3 J mol^{-1} K^{-1} [40]. Except for a sudden jump at the critical temperature, our results are also in good agreement with the experimental results at low temperature ($\leqslant$10 K) reported by He *et al* [2]. Furthermore, we find that when the temperature is below 300 K, the heat capacity C_V is strongly dependent on temperature, which is due to the anharmonic approximation. However, at higher temperatures, the anharmonic effect on C_V is suppressed, and C_V is almost constant at high temperature. The calculated dependences of C_V on temperature at different pressures do not show any anomalous behavior in the temperature range of 0–800 K and are similar to the superconducting compounds belonging to the conventional superconductors group.

In figure 5, the variation of Grüneisen parameter γ with pressure and temperature are displayed, from which it can be found that the Grüneisen parameter γ decreases exponentially

as the pressure increases just like the behavior of thermal expansion coefficient α, however, as the pressure enhanced the effect of temperature becomes more and more weak and the three curves representing 0, 500, 800 K almost converge together. Such a phenomenon is shown more clearly in the right part of figure 5, which displays the dependence of Grüneisen parameter γ on temperature. At zero pressure the Grüneisen parameter γ obviously increases with temperature, but at 30 and 55 GPa the tendency to increase becomes less.

3.5. Superconducting temperature

From the calculated pressure dependence of Debye temperature and $N(E_F)$ of total DOS, one can give an analysis of the positive dT_c/dP which is still controversial. In the BCS strong coupling limit, the superconducting temperature T_c is expressed by the McMillan formula [48]

$$T_c = \frac{\Theta}{1.45} \exp\left[-\frac{1.04(1+\lambda)}{\lambda - \mu^*(1+0.62\lambda)}\right], \qquad (17)$$

where μ^* denotes the Coulomb pseudopotential, which describes the repulsive interaction between electrons, λ is electron–phonon coupling constant, given by $\lambda = N(E_F)\langle I^2\rangle/M\langle\omega^2\rangle$, $\langle I^2\rangle$ is the average over the Fermi surface of square of the electronic matrix element for electron–phonon interaction, M is the ionic mass, and $\langle\omega^2\rangle$ is the square averaged phonon frequency. If $\lambda = 0.79$ and $\mu^* = 0.15$ [49] are taken, together with the Debye temperature $\Theta = 283.7$ K calculated by us in the GGA scheme, we obtain the critical temperature T_c equals to 7.3 K, consistent with other data [2, 49, 50].

It is noted that in equation (17) the critical temperature T_c is strongly dependent on Debye temperature, however, the dependence is complicated as it appears both in the linear and exponential term (from the $\langle\omega^2\rangle$ term in the expression of λ, as $\langle\omega^2\rangle = 0.5\Theta^2$). In order to investigate how the variation of the Debye temperature affects the dependence of T_c on pressure, we assume other variables, i.e. $N(E_F)$, $\langle I^2\rangle$ and μ^* are constants, with $\mu^* = 0.15$, and then make a numerical analysis. As the pressure applied changes from 0 to 58.4 GPa, the Debye temperature (calculated in GGA) increases from 283.7 to 377.3 K giving a positive factor making T_c grow to be about 1.33 T_c in the linear term. On the other hand, in the exponential term, the enhancement of Θ decreases λ to about 0.56 λ, which in turn makes T_c fall to about 0.079 T_c (assuming the initial value of λ is 0.79). Thus it is obvious that the change of Θ in the exponential term will be much more effective than that in the linear term in determining T_c. Synthetically, although with the same dependence of T_c on pressure, the enhancement of Debye temperature plays a negative role in the pressure dependence of T_c. Moreover, the $N(E_F)$ actually decreases with increasing pressure, which will also decrease the T_c. So if μ^* is less pressure dependent, the change of electronic contribution in electron–phonon interaction induced by pressure should make a positive contribution to the increase of T_c, i.e. as the pressure enhanced $\langle I^2\rangle$ increases.

4. Conclusions

In summary, the elastic properties of the non-oxide perovskite type superconductor $MgCNi_3$ under pressure have been investigated by first-principles calculations for the first time. With the local density approximation as well as the generalized gradient approximation for exchange and correlation, the ground state properties and equation of state of $MgCNi_3$ were obtained, which agree well with both theoretical calculations and experiments. From the high pressure elastic constants, we predict that $MgCNi_3$ is not stable at a pressure above 58.4 GPa and remains elastic anisotropic in the whole range of pressure studied. Furthermore, some thermodynamic properties such as the heat capacity and Grüneisen parameter are investigated under different pressures and temperatures. From analysis of the variation of Debye temperature and $N(E_F)$ with T_c, we conclude that $\langle I^2\rangle$ will increase with increasing pressure, which leads to a positive dT_c/dP for $MgCNi_3$.

Acknowledgments

The authors would like to acknowledge the support by the National Natural Science Foundation of China under Grant Nos 10776022, 10776029/A06 and 10576020, and by the State Key Program of National Natural Science of China under Grant No. 60436010.

References

[1] Nagamatsu J, Nakagawa N, Muranaka T, Zenaitani Y and Akimitsu J 2001 *Nature* **410** 63
[2] He T, Huang Q, Ramirez A P, Wang Y, Regan K A, Rogado N, Hayward M A, Haas M K, Slusky J S, Inumara K, Zandbergen H W, Ong N P and Cava R J 2001 *Nature* **411** 54
[3] Shim J H, Kwon S K and Min B I 2001 *Phys. Rev.* B **64** 180510
[4] Singh D J and Mazin I I 2001 *Phys. Rev.* B **64** 140507
[5] Dugdale S B and Jarlborg T 2001 *Phys. Rev.* B **64** 100508
[6] Szajek A 2001 *J. Phys.: Condens. Matter* **13** L595
[7] Shein I R, Ivanovskii A L and Medvedeva N I 2001 *JETP Lett.* **74** 122
[8] Rosner H, Weht R, Johannes M D, Pickett W E and Tosatti E 2002 *Phys. Rev. Lett.* **88** 027001
[9] Kumary T G, Janaki J, Mani A, Jaya S M, Sastry V S, Hariharan Y, Radhakrishnan T S and Valsakumar M C 2002 *Phys. Rev.* B **66** 064510
[10] Hayward M A, Haas M K, Ramirez A P, He T, Regan K A, Rogado N, Inumaru K and Cava R J 2001 *Solid State Commun.* **119** 491
[11] Klimczuk T and Cava R J 2004 *Solid State Commun.* **132** 379
[12] Das A and Kremer R K 2003 *Phys. Rev.* B **68** 064503
[13] Klimczuk T, Gupta V, Lawes G, Ramirez A P and Cava R J 2004 *Phys. Rev.* B **70** 094511
[14] Amos T G, Huang Q, Lynn J W, He T and Cava R J 2002 *Solid State Commun.* **121** 73
[15] Shan L, Xia K, Liu Z Y, Wen H H, Ren Z A, Che G C and Zhao Z X 2003 *Phys. Rev.* B **68** 024523
[16] Klimczuk T, Avdeev M, Jorgensen J D and Cava R J 2005 *Phys. Rev.* B **71** 184512
[17] Sulkowski C, Klimczuk T, Cava R J and Rogacki K 2007 *Phys. Rev.* B **76** 060501(R)
[18] Yang H D, Mollah S, Huang W L, Ho P L, Huang H L, Liu C J, Lin J Y, Zhang Y L, Yu R C and Jin C Q 2003 *Phys. Rev.* B **68** 092507

[19] Garbarino G, Monteverde M, Núñez-Regueiro M, Acha C, Weht R, He T, Regan K A, Rogado N, Hayward M and Cava R J 2004 *Physica* C **754** 408
[20] Loa I, Syassen K, Hanfland M, Zhang Y L, Yu R C and Jin C Q 2002 *Internal Report* MPI/FKF, Stuttgart (see poster under http://www.fkf.mpg.de/hd/)
[21] Zhang Y L, Li F Y, Chen L C, Liu J, Yu R C, Liu Z Y, Yu W and Jin C Q 2003 *Chin. Sci. Bull.* **48** 2287
[22] Kumar R S, Cornelius A L, Shen Y, Kumary T G, Janaki J, Valsakumar M C and Nicol M F 2005 *Physica* B **363** 190
[23] Vanderbilt D 1990 *Phys. Rev.* B **41** 7892
[24] Vosko S H, Wilk L and Nusair M 1980 *Can. J. Phys.* **58** 2100
[25] Perdew J P, Burke K and Ernzerhof M 1996 *Phys. Rev. Lett.* **77** 3865
[26] Parrinello M and Rahman A 1980 *Phys. Rev. Lett.* **45** 1196
[27] Parrinello M and Rahman A 1981 *J. Appl. Phys.* **52** 7182
[28] Payne M C, Teter M P, Allen D C, Arias T A and Joannopoulos J D 1992 *Rev. Mod. Phys.* **64** 1045
[29] Milman V, Winkler B, White J A, Packard C J, Payne M C, Akhmatskaya E V and Nobes R H 2000 *Int. J. Quantum Chem.* **77** 895
[30] Karki B B, Stixrude L, Clark S J, Warren M C and Ackland G J 1997 *J. Crain. Am. Mineral.* **82** 51
Wentzcovitch R M, Ross N L and Price G D 1995 *Phys. Earth Planet. Inter.* **90** 101
[31] Anderson O L 1963 *J. Phys. Chem. Solids* **24** 909
[32] Schreiber E, Anderson O L and Soga N 1973 *Elastic Constants and their Measurements* (New York: McGraw-Hill)
[33] Blanco M A, Francisco E and Luana V 2004 *Comput. Phys. Commun.* **158** 57
[34] Birch F 1947 *Phys. Rev.* **71** 809
[35] Vaitheeswaran G, Kanchana V, Svane A and Delin A 2007 *J. Phys.: Condens. Matter* **19** 326214
[36] Okoye C M I 2003 *J. Phys.: Condens. Matter* **15** 833
[37] Sieberer M, Mohn P and Redinger J 2007 *Phys. Rev.* B **75** 024431
[38] Heid R, Renker B, Schober H, Adelmann P, Ernst D and Bohnen K P 2004 *Phys. Rev.* B **69** 092511
[39] Tütüncü H M and Srivastava G P 2006 *J. Phys.: Condens. Matter* **18** 11089
[40] Zhou B, Wang R J, Zhang Y L, Li F Y, Yu R C and Jin C Q 2003 *Chin. J. High Pressure Phys.* **17** 157
[41] Frantsevich I N, Voronov F F and Bokuta S A 1983 *Elastic Constants and Elastic Moduli of Metals and Insulators Handbook* ed I N Frantsevich (Kiev: Naukova Dumka) p 60
[42] Sin'ko G V and Smirnow N A 2002 *J. Phys.: Condens. Matter* **14** 6989
[43] Oganov A R and Dorogokupets P I 2003 *Phys. Rev.* B **67** 224110
[44] Wälte A, Fuchs G, Müller K-H, Handstein A, Nenkov K, Narozhnyi V N, Drechsler S L, Shulga S, Schulty L and Rosner H 2004 *Phys. Rev.* B **70** 174503
[45] Kim I G and Lee J I 2002 *Phys. Rev.* B **65** 064525
[46] Shein I R, Ivanovskii A L, Kurmaev E Z, Moewes A, Chiuzbian S, Finkelstein L D, Neumann M, Ren Z A and Che G C 2002 *Phys. Rev.* B **66** 024520
[47] Szajek A 2001 *J. Phys.: Condens. Matter* **13** L595
[48] McMillan W L 1968 *Phys. Rev.* **167** 331
[49] Park M S, Giim J S, Park S H, Lee Y W, Lee S I and Choi E J 2004 *Supercond. Sci. Technol.* **17** 274
[50] Singer P M, Imai T, He T, Hayward M A and Cava R J 2001 *Phys. Rev. Lett.* **87** 257601